THE JOURNAL OF BIOLOGICAL CHEMISTRY
Vol. 279, No. 8, Issue of February 20, pp. 6824–6833, 2004
Printed in U.S.A.

The Kindler Syndrome Protein Is Regulated by Transforming Growth Factor-β and Involved in Integrin-mediated Adhesion*

Received for publication, July 22, 2003, and in revised form, November 19, 2003
Published, JBC Papers in Press, November 21, 2003, DOI 10.1074/jbc.M307978200

Susanne Kloeker‡, Michael B. Major‡, David A. Calderwood§, Mark H. Ginsberg§, David A. Jones‡, and Mary C. Beckerle‡¶‖

From the Departments of ‡Oncological Sciences and ¶Biology, Huntsman Cancer Institute, Salt Lake City, Utah 84112-5550 and §Department of Cell Biology, The Scripps Research Institute, La Jolla, California 92037

Transforming growth factor-β1 (TGF-β1) contributes to tumor invasion and cancer progression by increasing the motility of tumor cells. To identify genes involved in TGF-β-mediated cell migration, the transcriptional profiles of human mammary epithelial cells (HMEC) treated with TGF-β were compared with untreated cells by cDNA microarray analysis. One gene up-regulated by TGF-β was recently named kindlerin (Jobard, F., Bouadjar, B., Caux, F., Hadj-Rabia, S., Has, C., Matsuda, F., Weissenbach, J., Lathrop, M., Prud'homme, J. F., and Fischer, J. (2003) *Hum. Mol. Genet.* 12, 925–935). This gene is significantly overexpressed in some cancers (Weinstein, E. J., Bourner, M., Head, R., Zakeri, H., Bauer, C., and Mazzarella, R. (2003) *Biochim. Biophys. Acta* 1637, 207–216), and mutations in this gene lead to Kindler syndrome, an autosomal-recessive genodermatosis. TGF-β stimulation of HMEC resulted in a marked induction of kindlerin RNA, and Western blotting demonstrated a corresponding increase in protein abundance. Kindlerin displays a putative FERM (four point one ezrin radixin moesin) domain that is closely related to the sequences in talin that interact with integrin β subunit cytoplasmic domains. The critical residues in the talin FERM domain that mediate integrin binding show a high degree of conservation in kindlerin. Furthermore, kindlerin is recruited into a molecular complex with the β_{1A} and β_3 integrin cytoplasmic domains. Consistent with these biochemical findings, kindlerin is present at focal adhesions, sites of integrin-rich, membrane-substratum adhesion. Additionally, kindlerin is required for normal cell spreading. Taken together, these data suggest a role for kindlerin in mediating cell processes that depend on integrins.

The survival of cancer patients with solid tumors decreases dramatically when tumors are invasive and have an increased likelihood of metastasizing to distal sites. The enhanced invasiveness of tumor cells is attributed to epithelial to mesenchymal transition (EMT),[1] (5–8) a normal biological process that is critical for wound healing and development. EMT is characterized by a change in cell shape from a polarized epithelial cell to a flattened fibroblast-like morphology, a decrease in cell-cell junctions concurrent with a decrease in E-cadherin expression, and an increase in cell motility (5, 6). Transforming growth factor-β1 (TGF-β) is a major contributor to tumor progression and metastasis (9–11), and several studies have shown that TGF-β promotes tumor cell invasiveness by promoting EMT (9, 12–15). Despite the key role established for TGF-β in stimulating EMT and tumor progression, the molecular mechanisms by which TGF-β promotes EMT have not been fully elucidated.

Microarray analysis of a TGF-β-responsive cell line, human mammary epithelial cells (HMEC), led us to identify kindlerin as a TGF-β-inducible gene. Kindlerin is mutated in Kindler syndrome, a rare autosomal-recessive genodermatosis (1, 3). Early in life patients with Kindler syndrome endure blistering of the skin and photosensitivity, which progresses to diffuse poikiloderma followed by cutaneous atrophy (16, 17). The clinical presentation of this disease is similar to patients with junctional epidermolysis bullosa harboring mutations in α_6 and β_4 integrin genes (18, 19).

Kindlerin (also known as URP1 for UNC-112 related protein 1 or kindlin) is a member of a newly recognized protein family, which also includes Mig-2 and URP2 (2, 3). An apparent kindlerin orthologue, UNC-112, has been studied in *Caenorhabditis elegans* (20). The *unc-112* gene is essential for embryogenesis, and it displays a genetic interaction with integrins (20). Because integrins play a critical role in mammalian cell adhesion and migration, we postulated that kindlerin may be involved in TGF-β-stimulated EMT through interactions with integrins.

Here we report that kindlerin expression is responsive to TGF-β levels, that kindlerin localizes in focal adhesions (integrin-rich signaling centers that integrate extracellular matrix attachment and cytoskeletal organization), and that kindlerin forms complexes with integrin β subunit cytoplasmic domains. Furthermore, cell spreading is perturbed upon reduction of kindlerin protein. Taken together with the observation that kindlerin is overexpressed in colon and lung carcinomas (2), our data support a role for kindlerin in mammalian cell adhesion and suggest that kindlerin may mediate TGF-β signaling in tumor progression via contributions to integrin-dependent cellular functions.

* This work was supported by National Research Service Award F32 20457 (to S. K.), the Multidisciplinary Cancer Research Training Program Grant T32 CA93247 (to S. K.), the Huntsman Cancer Foundation, the Willard L. Eccles Foundation, National Institutes of Health Grants GM50877 (to M. C. B.) and HL48728 (to M. H. G.), the American Heart Association Scientist Development grant (to D. A. C.), and the University of Utah DNA-Peptide Facility and Sequencing Facility Technical Support Grant CA42014. The costs of publication of this article were defrayed in part by the payment of page charges. This article must therefore be hereby marked "*advertisement*" in accordance with 18 U.S.C. Section 1734 solely to indicate this fact.

‖ To whom correspondence should be addressed: Huntsman Cancer Institute, 2000 Circle of Hope, University of Utah, Salt Lake City, UT 84112-5550. Tel.: 801-581-4485; Fax: 801-581-2175; E-mail: mary.beckerle@hci.utah.edu.

[1] The abbreviations used are: EMT, epithelial to mesenchymal transition; TGF-β1, transforming growth factor β; HMEC, human mammary epithelial cells; Mig-2, mitogen inducible gene-2; FERM, four point one ezrin radixin moesin; PH, pleckstrin homology; siRNA, small interfering siRNA; PBS, phosphate-buffered saline; MES, 4-morpholineethanesulfonic acid; BisTris, 2-[bis(2-hydroxyethyl)amino]-2-(hydroxymethyl)propane-1,3-diol; PH, pleckstrin homology.

EXPERIMENTAL PROCEDURES

Cell Culture and Drug Treatments—HaCaT cells were maintained in Dulbecco's modified Eagle's medium supplemented with 10% fetal bovine serum and were split every 3rd day or at 80% confluency. The HaCaT immortalized keratinocyte cell line was a gift from D. Grossman. HMEC were obtained from BioWhittaker and cultured in complete mammary epithelial growth media. HMEC were seeded at passages 7 or 8 and harvested at no greater than 80% confluency for all experiments.

cDNA Microarray Data Analysis—The construction of the microarrays, generation of the microarray probes, microarray hybridization, and scanning were performed as described previously (21). First-strand cDNAs were generated by reverse transcription from the mRNA samples in the presence of Cy-3dCTP or Cy-5dCTP. The resulting labeled cDNAs were combined and simultaneously hybridized to the microarray slide displaying 4608 randomly selected and minimally redundant cDNAs from the unigene set (22). Each of the 4608 minimally redundant genes was present in duplicate on the microarray, and the comparisons were completed three separate times resulting in a total of six measurements for each gene. In each case, mRNA from TGF-β-treated cells was directly compared with mRNA from vehicle-treated cells. The GeneSpring software program (version 5.1; Silicon Genetics) was utilized for all steps in the data analysis. To normalize the microarray data, a Lowess curve was fit to the log intensity *versus* log ratio plot. 20.0% of the data was used to calculate the Lowess fit at each point. This curve was used to adjust the control value for each measurement. We selected TGF-β-responsive genes based on a statistical analysis using the gene expression program GeneSpring (version 5.1). We applied the inclusion criteria of 1.5-fold induction, and a p value of less than 0.05 (Student's t test) in defining TGF-β up-regulated genes. The list of genes shown in Table I was selected from the total normalized data set as having a fold induction greater than 1.5 in at least 4 of 6 data points (see the experimental description within Table I). Genes with a p value (Students t test) greater than 0.05 were not included. DNA sequencing and BLAST analysis confirmed the identity of each microarray clone corresponding to those genes listed in Table I.

Northern Blotting—For treatments with TGF-β1 (PeproTech), HMEC cells were not serum-starved prior to the addition of growth factor. The vehicle control for TGF-β1 was composed of 4 mM HCl, 1 mg/ml bovine serum albumin. Cycloheximide (Calbiochem) was used at 10 μg/ml and was added to the cells 15 min prior to the addition of TGF-β. Total RNA was isolated using Trizol (Invitrogen) followed by poly(A) RNA selection using a Poly(AT) Tract mRNA Isolation kit (Promega). Poly(A) RNA was fractionated through formaldehyde-containing agarose gels and transferred onto nylon membranes (Amersham Biosciences). Probes were generated using the Rediprime II random prime labeling system (Amersham Biosciences) supplemented with [^{32}P]dCTP. Hybridizations with ^{32}P-labeled probes were carried out using ULTRAhyb buffer (Ambion) as recommended by the manufacturer. The kindlerin probe was generated by amplification of the insert of a cDNA image clone (accession number 299593) using T7 and T3 primers.

Construction of FLAG-tagged Kindlerin cDNA—In order to manufacture the longest piece of the 5′ end of kindlerin cDNA, the EcoRI/SwaI fragment of AA158566 was subcloned into the EcoRI/SwaI sites of AI147142 to make clone A. Clone A was used as a template for PCR to add an EcoRI site directly 5′ of the ATG (sense oligonucleotide 5, 5′-ACG AAT TCA ATG CTG TCA TCC ACT GAC TTT AC-3′) and ended at the native PstI site (antisense oligonucleotide 6, 5′-CGA GGA TGC TGC AGT TTT GTT CC-3′). The EcoRI/PstI insert from clone A was excised and replaced with the PCR product digested with EcoRI/PstI in order to remove the 5′-untranslated region to generate clone B. The 3′ end of kindlerin cDNA was isolated by reverse transcriptase-PCR using RNA isolated from HMEC treated with TGF-β. The sense oligonucleotide 7 (5′-ATA GGT ACC TCA ATC CTG ACC GCC GGT CAA-3′) began at the HaeII site, and the antisense oligonucleotide 8 (5′-GAA GCG GCG CTT TCT AAT TTG GA-3′) added a KpnI site directly 3′ of the stop codon. The complete FLAG-kindlerin cDNA was assembled by three-piece ligation containing clone B digested with EcoRI and HaeII, the reverse transcriptase-PCR product digested with HaeII and KpnI, and FLAGpCMV2 digested with EcoRI and KpnI.

Kindlerin Antibody Generation—A construct expressing the C-terminal third of kindlerin (amino acid residues 500 to end) with a His tag was engineered as follows: a PCR product was generated using sense oligonucleotide 11 (5′-GCT CCA TAT GAT TCT TTC CTT TCT GAA GAT GCA GCA T-3′) and antisense oligonucleotide 12 (5′-ATG CGG CCG CTC ACA CCC AAC CAC TGG TAA GTT T-3′) using the FLAG-kindlerin cDNA as template and cloned into NdeI and NotI sites of the pET28a vector (Novagen). The construct was verified by DNA sequencing and utilized to transform competent BL21 cells (Novagen). The recombinant His-tagged kindlerin fragment was purified under denaturing conditions in 6 M urea. Fractions containing purified protein were pooled and concentrated using a Centricon-30 (Millipore). Concentrated protein was loaded onto SDS-PAGE, briefly stained with BioSafe Coomassie Blue (Bio-Rad), and excised from the gel. Gel pieces containing kindlerin were used to inject rabbits for polyclonal antibody production (Harlan Bioproducts for Science).

Western Blotting—For the TGF-β time course, HMEC or HaCaT were treated with vehicle or TGF-β (2 ng/ml) for the indicated times. Protein lysates were harvested from HaCaT or HMEC in a buffer containing 25 mM Tris-HCl, pH 7.4, 150 mM NaCl, 1 mM $CaCl_2$, 1% Triton X-100, 0.1 mM phenylmethylsulfonyl fluoride, 0.1 mM benzamidine, 1 mg/ml pepstatin A, and 1 mg/ml phenanthroline. The lysates were centrifuged at 20,800 × g for 10 min at 4 °C. The supernatant was transferred to a clean tube and assayed for protein concentration using the DC Protein Assay (Bio-Rad). For antibody characterization (Fig. 3*A*), lysates were heated at 70 °C for 10 min in LDS sample buffer (Invitrogen) and then separated by Tris-glycine 10% SDS-PAGE and transferred to nitrocellulose (Millipore). The blots were incubated with indicated kindlerin, vinculin (Sigma), or E-cadherin (Transduction Laboratories) antibodies, followed by incubation with donkey anti-rabbit horseradish peroxidase or sheep anti-mouse horseradish peroxidase (Amersham Biosciences). Immune complexes were visualized with Western Lightning Chemiluminescence Reagent (PerkinElmer Life Sciences). For the time course experiments, lysates were harvested and analyzed as indicated above, with the exception that BisTris 4–12% NuPAGE using MES running buffer (Invitrogen) was utilized to separate the lysates.

Phase Contrast Imaging—HMEC were allowed to adhere overnight and were subsequently treated with vehicle or TGF-β for 48 h. Cell morphology was observed using a Nikon microscope and recorded with a digital camera.

Affinity Purification of Kindlerin Antibody and Indirect Immunofluorescence—Kindlerin antiserum was affinity-purified by using a method described previously (23). Briefly, antiserum was incubated with recombinant kindlerin immobilized on nitrocellulose. After extensive washing of the membrane, the bound antibodies were eluted with 100 mM glycine, pH 2.5, and immediately combined with 1 M Tris-HCl, pH 9.0, sufficient to neutralize the glycine-HCl. The eluted material was then concentrated in a Centricon-10 device (Amicon). The control antibody was absorbed to nitrocellulose without kindlerin protein. Indirect immunofluorescence was performed by plating HaCaT cells on glass coverslips coated with 10 μg/ml fibronectin (Sigma) in Dulbecco's modified Eagle's medium (Invitrogen) supplemented with 10% fetal bovine serum (Invitrogen). To examine kindlerin localization in the presence of TGF-β, cells were treated with vehicle or TGF-β (2 ng/ml) for 48 h. Coverslips were washed in PBS, fixed for 15 min with 4% formaldehyde, 5 μM $CaCl_2$, 0.5 μM $MgCl_2$ in PBS, and permeabilized for 4 min with 0.2% Triton X-100 in PBS. After washing in PBS, the coverslips were incubated with primary antibodies at 37 °C for 120 min, washed in PBS for 10 min, and subsequently incubated with Alexa-488- or Alexa-594-conjugated secondary antibodies (Molecular Probes). The coverslips were mounted with ProLong (Molecular Probes) after washing for 10 min in PBS. Primary antibodies used in this study include affinity-purified rabbit polyclonal kindlerin antibody R-2230 (1:100), control antibody (1:100), rabbit polyclonal talin antibody B-11 (1:800), and vinculin monoclonal antibody (1:300 Sigma). Actin filaments were visualized using Alexa-488-conjugated phalloidin (1:100 Molecular Probes). Cell images were visualized on a Zeiss Axiophot microscope and recorded with a digital camera.

Kindlerin and Talin Amino Acid Alignment and Modeling—The primary sequences of kindlerin and talin were aligned by blast searching (www.ncbi.nlm.nih.gov/blast/) and refined using structure-based alignments performed by Swiss-PdbViewer (us.expasy.org/spdbv/) using the structure of talin subdomains F2 and F3 (4) (Protein Data Bank code 1MK7) as template. Based on the sequence alignment, the putative kindlerin F3 subdomain (residues 566–655) was modeled on the talin F3 subdomain (residues 309–400 from Protein Data Bank code 1MK7). Modeling was performed using Swiss model (24–26), and the quality of the resulting model was assessed using WHAT_CHECK and WHAT-IF version 19970813-1517 (27, 28).

Integrin β Tail Binding Assays—Affinity chromatography was performed by using recombinant models of integrin cytoplasmic tails as described previously (29). Briefly, Chinese hamster ovary cells transfected with FLAG-kindlerinpCMV2 were lysed as described previously (29), and the indicated amount of lysate was mixed with 50 μl of

TABLE I
Genes Induced by TGF-β in HMEC

Human mammary epithelial cells were treated with TGF-β (10 ng/ml) for 3 h; mRNA harvested from treated and non-treated HMEC samples (3 independent replicates) was reverse-transcribed into cDNA in the presence of either a green or red fluorescent tag. Competitive hybridization of the labeled cDNAs on glass slides containing 4608 cDNAs spotted in duplicate revealed the relative increase and decrease of specific mRNAs. Stringent data analysis (greater than 1.5-fold in 4 of the 6 microarray ratios; *p* value less than 0.05) facilitated the identification of 17 TGF-β up-regulated transcripts.

Gene name	Fold change	*p* value[a]
Plasminogen activator inhibitor, type I (PAI1)	3.07	7.76E-07
Integrin α_2	2.55	4.46E-04
Kindlerin	2.30	5.36E-05
Transglutaminase	2.17	5.07E-03
TGF-β induced, 68-kDa	1.96	4.92E-03
Connective tissue growth factor	1.94	4.32E-05
PMEPA1	1.89	5.56E-03
Sox-4	1.88	1.66E-02
Tubulin α-4 chain	1.76	2.13E-02
Tis11D/ERF-2	1.70	3.22E-04
Gadd45β	1.69	7.24E-04
EST (accession no. Al828370)	1.66	6.81E-03
DNA G/T mismatch-binding protein	1.63	6.79E-05
Thrombospondin 1	1.62	1.68E-02
TGF-β inducible early protein (TIEG)	1.61	4.04E-05
Early growth response (EGR-1)	1.58	3.63E-02
Fibronectin	1.58	8.22E-05

[a] *p* values were calculated using the Student's *t* test from 6 independent microarray expression ratios.

His-Bind resin coated with recombinant integrin tails. Beads were washed and bound proteins fractionated by SDS-PAGE, and kindlerin was detected by Western blotting with FLAG antibodies. Loading of recombinant integrin tails onto the beads was assessed by Coomassie Blue staining.

siRNA Transfection—HaCaT cells were transfected using siPORT Amine (Ambion) with a 21-nucleotide irrelevant RNA (control) or with a 21-nucleotide RNA targeting the kindlerin sequence (only sense sequence is shown): 5′-GAA GUU ACU ACC AAA AGC UTT. Cells were harvested ~44 h after adding siRNA duplexes and examined for kindlerin expression by Western blot analysis. To show equivalent loading of protein, the membrane was probed with a talin monoclonal antibody (Sigma).

Cell Spreading—Approximately 44 h after addition of the siRNA duplexes, cells were trypsinized and washed 2 times in Opti-MEM (Invitrogen). Cells were plated on fibronectin (10 μg/ml, Sigma)-coated coverslips and were allowed to spread for 30 min at 37 °C, 5% CO_2. Cells were stained by indirect immunofluorescence as described above using talin and vinculin antibodies. A minimum of four randomly selected fields (~180 cells total) was recorded with a digital camera. The area of cell spreading visualized by talin immunofluorescence was measured using Openlab software.

RESULTS

TGF-β Treatment Increases Kindlerin Expression—TGF-β elicits its biological effects by activation of a SMAD-dependent transcriptional program (reviewed in Refs. 30–33). To identify potential downstream targets of TGF-β signaling that are involved in EMT and cell migration, we used microarray analysis to compare the transcriptional profiles of HMEC treated with 10 ng/ml TGF-β to those of vehicle-treated cells. Seventeen genes exhibited a greater than 1.5-fold induction and a *p* value of less than 0.05 (Table I). Induced genes included a number of known TGF-β-responsive genes with roles in cell motility and adhesion such as plasminogen activator inhibitor type I (34, 35), transglutaminase (36), thrombospondin 1 (37), and fibronectin (35). We examined Table I for novel genes with predicted roles in cell adhesion and migration, and we recognized that the third ranking gene encoded kindlerin, a protein required for stable attachment of epithelial cells to the lamina densa (1). Kindlerin displays similarity throughout its sequence to two other human proteins, Mig-2 (65% identity) and URP2 (57% identity), as shown in Fig. 1 and appears to be related to the *C. elegans* protein, UNC-112 (44% identity). UNC-112 is required for the organization of dense bodies and attachment of muscle cells to the hypodermis, and UNC-112 interacts genetically with integrins (20). Thus we focused on kindlerin as a possible mediator of TGF-β effects on integrin function.

In order to verify the induction of the kindlerin gene by TGF-β, mRNA was isolated every 2 h up to 12 h after treatment with TGF-β and examined by Northern blot analysis for kindlerin expression (Fig. 2*A*). A 4.6-kb kindlerin mRNA transcript was induced ~10-fold 6 h after addition of TGF-β. The level of kindlerin transcript remained elevated after exposure to TGF-β for 96 h (data not shown). To examine the role of protein synthesis in regulation of kindlerin mRNA, we examined the effect of cycloheximide on TGF-β stimulated HMEC. Kindlerin mRNA abundance was markedly increased by the addition of TGF-β (Fig. 2*B*). Addition of cycloheximide significantly reduced the effect of TGF-β on kindlerin mRNA, indicating that protein synthesis is required for the TGF-β stimulation of kindlerin transcription. Thus, kindlerin is a TGF-β-inducible gene.

We next assessed the effect of TGF-β on the abundance of the kindlerin protein. We raised polyclonal antibodies directed against a bacterially expressed protein fragment containing amino acids 500–677. Western immunoblot analysis shows that the kindlerin antiserum specifically recognizes a protein with an apparent molecular weight of 64,000 (Fig. 3*A*) in HMEC and HaCaT lysates. Because HaCaT and HMEC respond to TGF-β and express kindlerin, these cell lines were used for our studies of the endogenous protein. The antiserum did not recognize two kindlerin paralogues, Mig-2 and URP2, in mouse fibroblasts transfected with FLAG-Mig-2 or FLAG-URP2 cDNA (data not shown); therefore, the antiserum is specific for kindlerin.

To determine whether TGF-β increases kindlerin protein levels, HMEC (Fig. 3*B*) and HaCaT cells (data not shown) were treated with TGF-β, and lysates were prepared at various time points up to 48 h after initiation of treatment. Kindlerin levels increased slightly at 8 h, significantly at 24 h, and most dramatically at 48 h after TGF-β treatment. The induction of kindlerin by TGF-β reached a plateau at 48 h and remained elevated for up to 96 h (data not shown). The membrane was stripped and probed with vinculin antibodies to normalize for equal protein levels. Kindlerin expression was quantitated relative to vinculin abundance at the indicated time points (Fig. 3*C*). Probing a parallel blot with E-cadherin antibodies showed a decrease in expression upon TGF-β treatment, which is indicative of cells undergoing EMT. Additionally, exposure of HMEC to TGF-β for 48 h induces a change from a round, compact epithelial shape to a flattened fibroblast-like morphology (Fig. 3*D*). This change in morphology is consistent with those observed for cells undergoing EMT in response to TGF-β. These results demonstrate that kindlerin levels increase in the presence of TGF-β and indicate that kindlerin may act as a downstream mediator of TGF-β-initiated EMT.

Kindlerin Is a Constituent of Focal Adhesions—EMT results in increased cell motility and a reorganization of the cytoskeleton (5, 6). The kindlerin orthologue, UNC-112, co-localizes with integrin adhesion receptors at dense bodies in the body wall muscle of *C. elegans* and is required for the proper organization of integrin complexes at the site of muscle attachment to the hypodermis (20). Dense bodies in worms and focal adhesions in mammalian cells share many common components (38). To determine whether kindlerin is targeted to focal adhe-

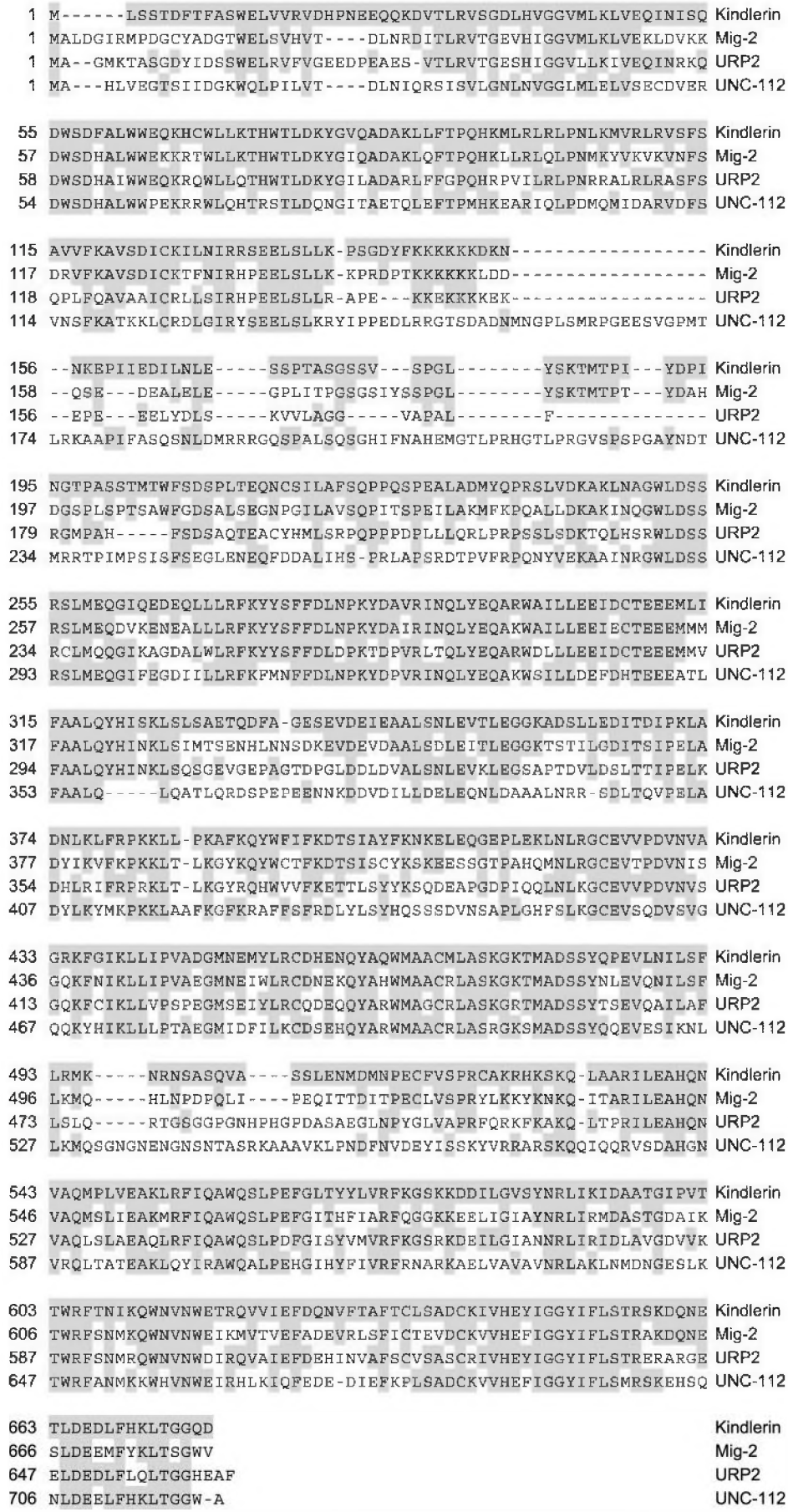

FIG. 1. **Comparison of the amino acid sequences of kindlerin paralogues and UNC-112.** Amino acid alignment of kindlerin, Mig-2, URP2, and UNC-112. Identical amino acids are highlighted in *black*, and *dashes* indicate gaps in the alignment. The amino acid sequences were aligned using the Clustal method.

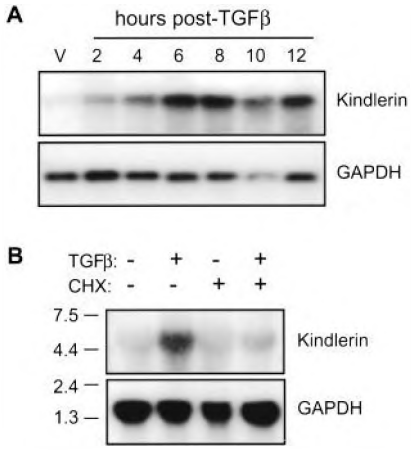

FIG. 2. **TGF-β treatment of HMEC.** *A*, Northern blot analysis of kindlerin and GAPDH using mRNA isolated from HMEC treated with vehicle (*V*) or TGF-β for the indicated time. *B*, HMEC were treated with vehicle (−) or TGF-β (+) for 3 h, and total RNA was isolated. In parallel cultures, cycloheximide (*CHX*) was added to the cells 15 min prior to the addition of TGF-β. Expression levels of kindlerin and GAPDH were analyzed by Northern blot.

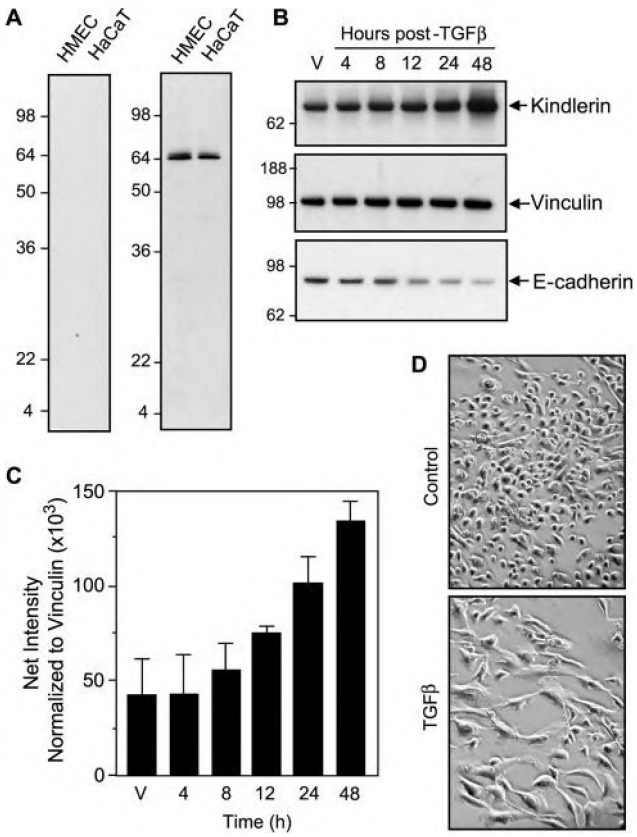

FIG. 3. **Antibody characterization and kindlerin expression in TGF-β-treated HMEC.** *A*, Western blot analysis of HMEC and HaCaT lysates (25 μg) using pre-immune (*left panel*) or kindlerin antiserum (*right panel*). *B*, time course analysis of HMEC treated with TGF-β. Lysates (15 μg) were probed with kindlerin, vinculin, and E-cadherin antibodies. *C*, quantification of kindlerin induction by TGF-β normalized to vinculin levels. *D*, phase contrast images of HMEC treated with vehicle (*control*) or TGF-β for 48 h. Images were taken at the same magnification.

sions in mammalian cells, immunofluorescence was performed using an affinity-purified kindlerin antibody to detect endogenous kindlerin. As can be seen in Fig. 4, kindlerin was concentrated in focal adhesions where it co-localizes with vinculin. Vinculin and integrin adhesion receptors are co-localized at

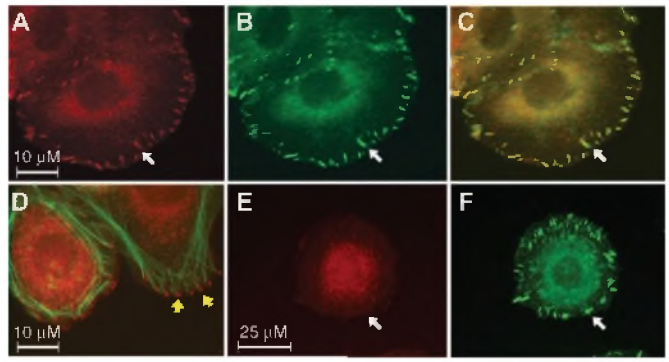

FIG. 4. **Localization of kindlerin in mammalian cells.** Indirect immunofluorescence analysis of HaCaT cells using kindlerin (*A*) and vinculin (*B*) antibodies. *C* is a merged image of *A* and *B*. *White arrows* indicate sites of focal adhesions. *D* shows combined staining of kindlerin (*red*) and F-actin (*green*). *Yellow arrows* point to kindlerin localization at the ends of actin filaments. HaCaT cells stained with control (*E*) and vinculin (*F*) antibodies.

focal adhesions in several cell types, including specialized epithelial cells such as keratinocytes (39–43). Visualization of filamentous actin by fluorescent phalloidin demonstrated that kindlerin is present at the tips of actin fibers (Fig. 4*D*). No focal adhesion staining was detected with a control antibody (Fig. 4*E*) even though focal adhesions are present and observed using a vinculin antibody (Fig. 4*F*). Kindlerin was not detected at cell-cell junctions that were compared by staining with E-cadherin antibodies (data not shown). Thus, kindlerin is a constituent of focal adhesions.

Kindlerin Localizes to Membrane Ruffles upon TGF-β Treatment—Our data show that kindlerin is a focal adhesion protein whose expression is regulated by TGF-β. In order to gain insight into the role of kindlerin in TGF-β-mediated cytoskeletal reorganization, we examined its localization in HaCaT cells exposed to vehicle (Fig. 5, *A* and *B*) or TGF-β (Fig. 5, *C* and *D*) and co-stained with fluorescent phalloidin. After 48 h of TGF-β stimulation, a marked increase in cell spreading occurred, indicative of the transition from an epithelial to a mesenchymal cell morphology. In vehicle-treated cells, the actin cytoskeleton was organized as a network of filaments that circumscribes each cell colony. After exposure to TGF-β, actin filaments were reorganized to establish actin arrays that are typical of fibroblastic cells. A fraction of kindlerin remained in focal adhesions and localized to the ends of actin fibers, but there was a notable increase in kindlerin expression in a more diffuse cytoplasmic staining pattern. Co-staining HaCaT cells with kindlerin and vinculin antibodies revealed a differential responsiveness of these two focal adhesion constituents to TGF-β treatment (Fig. 6). After TGF-β treatment, a significant loss of coincidence of kindlerin and vinculin was observed in many but not all focal adhesions (Fig. 6, *D–I*). TGF-β resulted in an enrichment of kindlerin in membrane ruffles particularly at sites of contact with other cells. The focal adhesion constituent, vinculin, remained present at extracellular matrix attachment sites indicating that focal adhesions had not been dissolved.

FERM Domain of Kindlerin Is Highly Similar to the FERM Domain of Talin—As described above, kindlerin localizes to focal adhesions, and analysis of the kindlerin amino acid sequence suggests a rationale for this localization. A search for conserved domains revealed that a striking feature of kindlerin is homology of two regions of the protein with the FERM (four point one ezrin radixin and moesin) domain (Fig. 7*A*, *gray*, *green*, and *blue boxes*) and a predicted pleckstrin homology domain (Fig. 7*A*, *black box*). Interestingly, the pleckstrin homology domain sits in the middle of a putative contiguous FERM domain, and this architecture is a unique hallmark

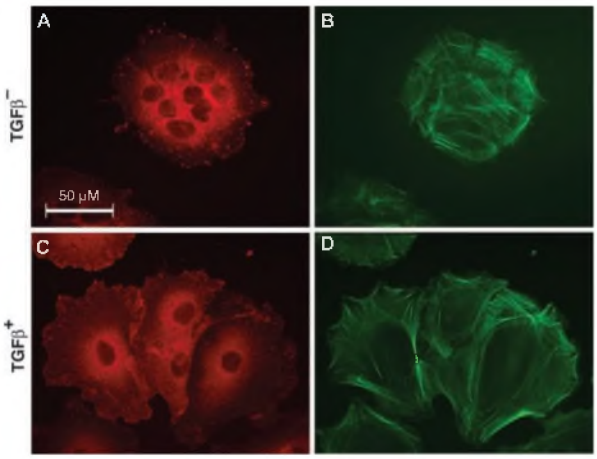

FIG. 5. **The effect of TGF-β treatment on kindlerin distribution and the actin cytoskeleton.** Staining patterns of kindlerin (*red*) and F-actin (*green*) in the absence (*A* and *B*) and presence (*C* and *D*) of TGF-β in HaCaT cells. The images in *A–D* are shown at the same magnification, and the *bar* indicates 50 μM.

shared by the members of the kindlerin family including Mig-2 and URP2.

Among other FERM domain proteins, the kindlerin FERM domain has the highest similarity to the FERM domain of talin (44), an integrin-binding protein that localizes to focal adhesions (29). In order to gain insight into the function of the FERM domain of kindlerin, we aligned the amino acid sequence of these corresponding regions in talin and kindlerin (Fig. 7*B*). The *gray box* at amino acid 250 in kindlerin (Fig. 7*A*) illustrates where the similarity to talin begins. FERM domains are composed of three subdomains (F1, F2, and F3) arranged in a cloverleaf pattern (45) and often mediate interactions with the cytoplasmic domains of transmembrane proteins. The regions similar to the F2 and F3 subdomains of talin are indicated by *green* and *blue*, respectively. The structure of the F2 and F3 subdomains of talin has been solved (4), and alignment of kindlerin and talin FERM domains predicts that the PH domain lies in the large loop between the second and third α-helix of the F2 subdomain. In talin, this region does not compose any of the core structure of the F2 domain. PH domains (Conserved Domain data base: smart00233) can be inserted into other domains that retain activity (www.ncbi.nlm.nih.gov/Structure/cdd/); therefore, it is plausible that kindlerin houses a functional PH domain within a structurally intact FERM domain.

The mutations identified in Kindler syndrome (as indicated by *asterisks* in Fig. 7*A*) yield truncated forms of kindlerin, all of which compromise the integrity of the FERM domain (1). The longest disease-associated gene product is predicted to generate a protein identical to kindlerin through the first 572 (*arrow* in Fig. 7*B*) amino acids followed by three unique amino acids (1). The resulting protein contains only five amino acids of the predicted F3 subdomain, indicating the essential role of the F3 subdomain for kindlerin function.

The sequence similarities between F3 subdomains of talin and kindlerin permitted us to build a reliable three-dimensional model of the kindlerin F3 subdomain (Fig. 7*C*). As judged by the program WHAT-IF (27), the model has normal inside/outside distribution of hydrophobic/hydrophilic residues (Z score 1.005) and structural packing quality (Z score −1.135), and the Ramachandran Z score (−0.371) is within the range of well refined structures. Comparison of the model with talin F3 gives a root mean square of 1.32 Å for 88 Cα atoms. Thus, the phosphotyrosine binding-like fold of F3 subdomains is compatible with the sequence of the putative F3 subdomain of kindlerin.

The major integrin-binding site in talin lies within the F3 subdomain (46). Amino acids participating in this interaction (4) are *boxed* in Fig. 7*B*, and the corresponding amino acids in kindlerin are similar or identical. Modeling of the kindlerin F3 domain further highlights that many of the residues conserved between talin and kindlerin, indicated by the *teal color* in the kindlerin model, are clustered in the integrin binding region of the F3 subdomain (Fig. 7*C*).

β Integrin Cytoplasmic Domains Form Complexes with Kindlerin—The amino acid conservation between the talin and kindlerin FERM domains, particularly within the region responsible for binding to integrin β tails, led us to hypothesize that kindlerin may bind to integrins. To test this hypothesis, lysates from Chinese hamster ovary cells expressing exogenous FLAG-kindlerin were incubated with recombinant β integrin tails (Fig. 8*A*). Kindlerin was isolated with either the β_{1A} or β_3 integrin cytoplasmic domain. The association was specific as no kindlerin was isolated with the cytoplasmic domain of integrin α_{IIb}. Tyrosine to alanine mutations within the conserved integrin NPXY motifs, which are known to disrupt a β turn (47) required for talin binding (46), also significantly reduced kindlerin-integrin interactions. Furthermore, the binding of kindlerin to the cytoplasmic domain of integrin β_3 is dose-dependent (Fig. 8*B*). Maximum binding was observed with 50 μg of lysates. Hence, focal adhesion localization of kindlerin may be mediated by FERM domain-integrin β tail interactions.

Binding of F3 subdomain of talin to the cytoplasmic domains of β_3 integrins leads to an increase in integrin affinity for ligand (integrin activation) (46, 48). The similarity of kindlerin to the FERM domain of talin, in both amino acid sequence and ability to bind the cytoplasmic domain of β integrins, therefore prompted us to examine the effect of overexpressed kindlerin on $\alpha_{IIb}\beta_3$ activation. Kindlerin expression had no effect on $\alpha_{IIb}\beta_3$ activation (data not shown). This finding is similar to Numb and Dok1, other integrin β tail-binding proteins containing homology to the F3 domain of talin, which are also unable to activate integrins (46).

Kindlerin Is Involved in Cell Spreading—The preceding data show that kindlerin is an integrin-associated focal adhesion protein. To assess the function of kindlerin, we employed small interfering RNA (siRNA) duplexes to reduce the expression of kindlerin in human cells. Kindlerin protein was reduced in lysates prepared from HaCaT cells transfected with kindlerin siRNA as compared with lysates prepared from cells transfected with an irrelevant siRNA as shown by Western blot (Fig. 9*A*). The membrane was stripped and probed for talin to demonstrate equal protein levels in both lanes. Forty-four hours after transfection of the siRNA duplexes, cells were replated on fibronectin-coated coverslips and allowed to spread for 30 min. Indirect immunofluorescence analysis using talin antiserum revealed a decrease in the ability of kindlerin siRNA cells to spread as compared with control cells (Fig. 9*B*). To quantify the change in cell spreading, the cell area was measured for ~200 cells (Fig. 9*C*). The mean cell area was 712 μm^2 for control siRNA cells and 452 μm^2 for kindlerin siRNA cells. Thus, reduction in kindlerin levels affects cell spreading.

DISCUSSION

In this report, we have explored the molecular mechanisms underlying the cellular response to TGF-β. We present the following data: (i) kindlerin expression is increased following stimulation with TGF-β; (ii) kindlerin is a constituent of focal adhesions; (iii) the integrin-binding residues found in talin are conserved in kindlerin; (iv) kindlerin can be isolated in β integrin tail complexes; and (v) kindlerin is required for normal cell spreading.

We became interested in the kindlerin gene when examining

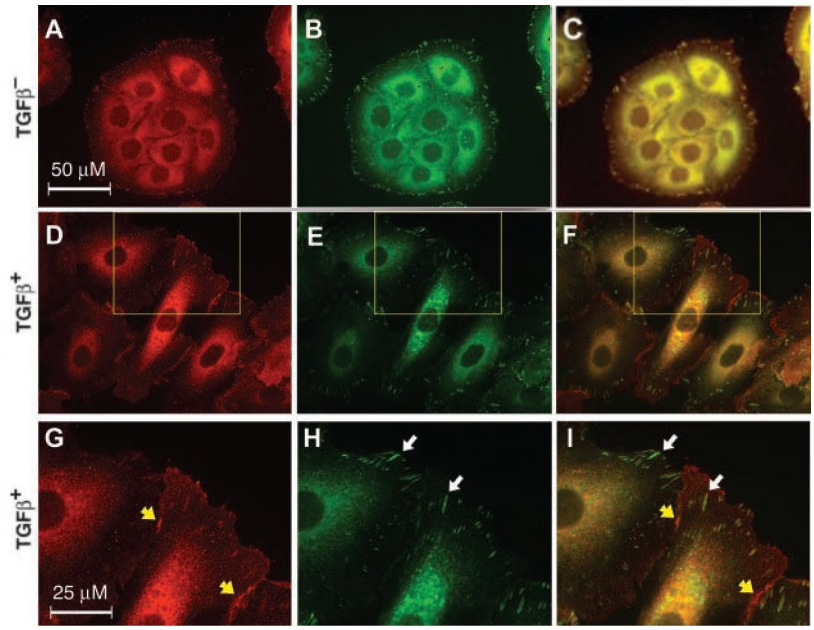

FIG. 6. **The effect of TGF-β treatment on kindlerin distribution and vinculin localization.** Indirect immunofluorescence analysis of kindlerin (*red*) and vinculin (*green*) in the absence (*A–C*) or presence (*D–I*) of TGF-β. The images in *A–F* are shown at the same magnification, and the *bar* indicates 50 μM. *G–I* represent enlarged images of the *boxed* regions in *D–F*. *Yellow arrows* indicate sites of kindlerin-enriched staining, and *white arrows* point to focal adhesions stained by vinculin antibodies.

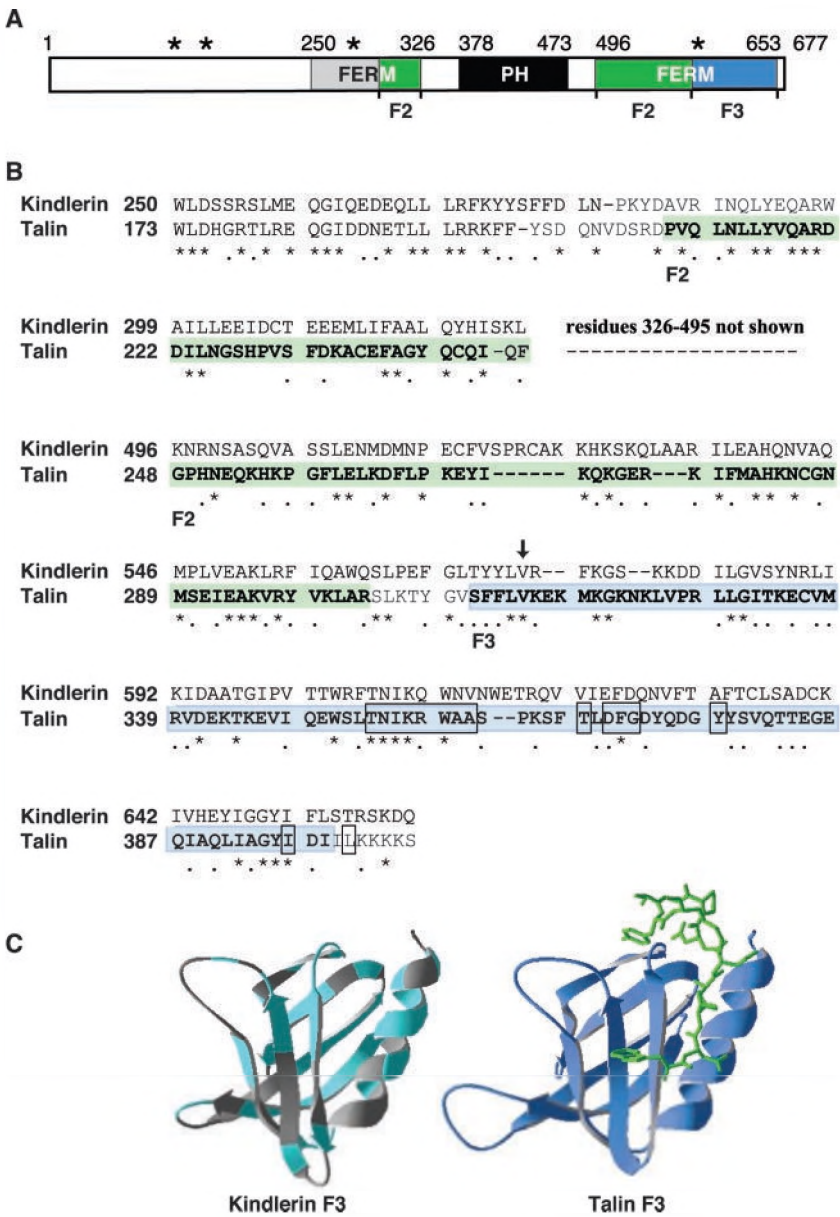

FIG. 7. **Comparison of talin and kindlerin FERM domains.** *A*, linear diagram of kindlerin. The FERM domain is shown in *green* and *blue* to indicate the F2 and F3 subdomains, respectively; and the *gray box* indicates homology to talin before the predicted start of the F2 subdomain. The PH domain is indicated by a *black box*. Mutations identified in Kindler syndrome by Jobard *et al.* (1) are indicated by *asterisks* at amino acids 128, 154, 262, and 572. *B*, alignment of kindlerin and talin FERM domains. The primary sequences of kindlerin and chicken talin were aligned by blast searching and refined using structure-based alignments performed by Swiss-PbdViewer (us.expasy.org/spdbv/). Identical residues are marked with * and similar residues with . *below the alignment*. The *arrow* indicates residue 572, site of one of the mutations identified in Kindler syndrome. The *boxed* residues in talin mediate the β integrin-talin interaction. Kindlerin exhibits sequence similarity to the talin FERM domain, and the talin FERM subdomains F2 and F3 are highlighted in *green* and *blue*, respectively. Kindlerin contains a large insertion, residues 326–495, containing a predicted PH domain, within the putative FERM domain. These amino acids are not shown in the alignment. *C*, model of the kindlerin F3 subdomain. Ribbon representations of the homology model of the kindlerin F3 subdomain (*left*) and of the talin F3 subdomain structure with the integrin ligand in *green* (Protein Data Bank code 1MK7; *right*). Regions of kindlerin exhibiting primary sequence similarity to talin are colored *teal*. Modeling was performed and the figure generated using Swiss-PdbViewer.

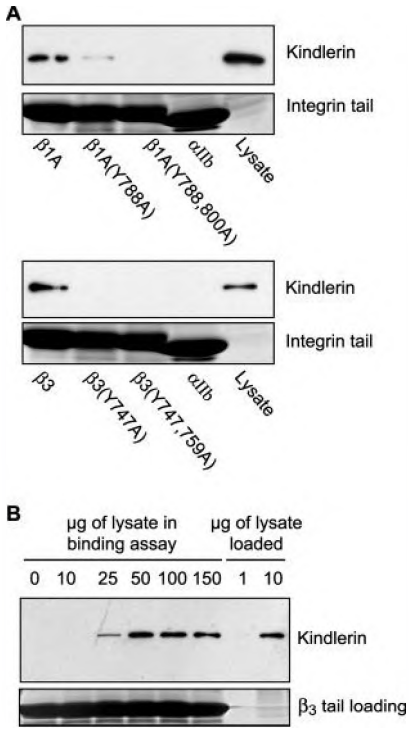

FIG. 8. **Integrin β tails form complexes with kindlerin.** *A*, cell lysate (150 μg) containing FLAG-tagged kindlerin was mixed with beads coated with recombinant integrin cytoplasmic tails or tails containing point mutations as indicated. Bound proteins were fractionated by SDS-PAGE and binding of kindlerin assessed by Western blotting with anti-FLAG antibodies. Loading of recombinant integrin tails onto the beads was assessed by Coomassie Blue staining. *B*, increasing amounts of cell lysate containing FLAG-tagged kindlerin were incubated with integrin tails and analyzed as in *A*.

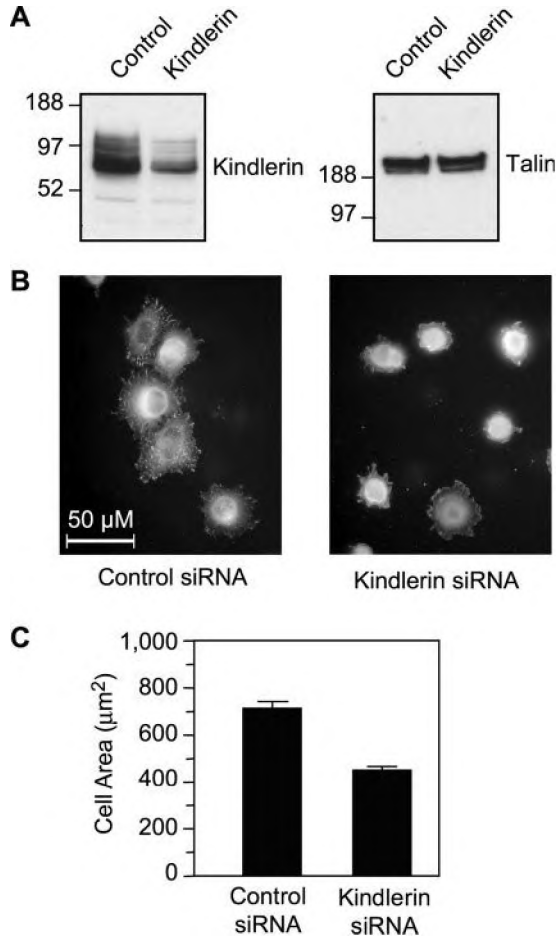

FIG. 9. **The effect of kindlerin knock-down on cell spreading.** *A*, Western blot analysis of lysate (20 μg) from control or kindlerin siRNA transfected HaCaT cells probed with kindlerin antiserum (*left panel*). The membrane was stripped and probed with talin antibodies (*right panel*) to demonstrate equivalent protein levels. *B*, indirect immunofluorescence analysis of control (*left panel*) or kindlerin (*right panel*) siRNA transfected HaCaT after plating on fibronectin-coated coverslips for 30 min using talin antiserum. *C*, the cell area of ~200 cells was measured by recording images of talin immunofluorescence. The *p* value is less than 0.0001 using a two-tailed unpaired *t* test. The data are representative of three independent experiments.

our microarray data for genes that may be involved in TGF-β-stimulated migration. Several pieces of circumstantial evidence prompted us to investigate a possible role for kindlerin in mammalian cell adhesion and migration. First, kindlerin contains two regions of homology with the FERM domain with a PH domain inserted inbetween the two. The FERM domain has been identified in several molecules such as ezrin, radixin, and moesin that connect the cytoplasmic domains of transmembrane proteins to the actin cytoskeleton (44). Other proteins that display FERM domains are involved in cell migration including focal adhesion kinase and talin (49). A second clue about the potential function of kindlerin stems from studies of an apparent orthologue in *C. elegans*, UNC-112. UNC-112 null worms exhibit the paralyzed arrested at 2-fold phenotype, a phenotype that is shared by α and β integrin, integrin-linked kinase, and perlecan (20). GFP-UNC-112 rescued embryonic lethality and co-localized with integrins at dense bodies in the body wall muscle (20). In the absence of UNC-112, α integrin failed to localize to the membrane in body wall muscle (20). Moreover, UNC-112 was not properly targeted to the membrane in worms lacking α integrin implying an interdependence of UNC-112 and α integrin for organization of dense bodies (20). The unique domain architecture of kindlerin and the elegant genetic studies of *unc-112* led us to hypothesize that kindlerin is involved in mammalian cell adhesion and migration.

We characterized kindlerin as a protein whose expression increases significantly in the presence of TGF-β. Our studies indicate that enhanced transcription of the kindlerin gene is most likely a secondary response to TGF-β stimulation because its induction is markedly reduced in the presence of the protein synthesis inhibitor cycloheximide. Additionally, peak levels of kindlerin mRNA and protein occurred at 6 and 48 h, respectively, after treatment with the cytokine. At 12 h when the levels of kindlerin began to increase, levels of E-cadherin, a marker for EMT, began to decline. Other reports have shown that EMT has taken place in HaCaT cells after 48 h of exposure to TGF-β (50), and the reduction of E-cadherin expression indicated that our cells were responding in a similar fashion. The increase in kindlerin levels occurred during the later stages of EMT progression, and these data suggest that kindlerin may be involved in the downstream events of the TGF-β response.

Indirect immunofluorescence analysis of kindlerin in HaCaT demonstrated that endogenous kindlerin localizes to focal adhesions in mammalian cells. After TGF-β stimulation, kindlerin is also detected at membrane ruffles particularly at sites of cell-cell contact. The presence of kindlerin at focal adhesions is consistent with its isolation in integrin complexes and implies a role in cell-matrix adhesion. A kindlerin-related protein, Mig-2, has also been shown to localize to focal adhesions and is involved in regulating cell shape and cell spreading (51). Mig-2 interacts with a protein termed migfilin, which potentially could connect Mig-2 to filamin and the actin cytoskeleton. The presence of Mig-2 at focal adhesions is consist-

ent with our findings on kindlerin and supports a general role for the Mig-2 family in cell adhesion. To date, no reports have described URP2 function; however, its high expression levels in spleen, thymus, and peripheral blood leukocytes suggest a role specific to the immune system (2). Future experiments will be needed to address the role of the enrichment of kindlerin at membrane ruffles and sites of cell-cell contact in altered adhesion, migration, and morphology of TGF-β-treated cells.

Based on the homology of the FERM domain of kindlerin with talin and the genetic interaction in *C. elegans* between UNC-112 and integrins, we suspected that kindlerin interacts with the cytoplasmic domain of the β integrin subunit. In support of this hypothesis, recombinant structural mimics of β_{1A} and β_3 integrin cytoplasmic domains were able to isolate exogenously expressed FLAG-kindlerin. Although these experiments do not demonstrate a direct interaction between kindlerin and β integrin, similarity with talin and the absence of kindlerin binding to the integrin β cytoplasmic domains containing tyrosine to alanine mutations suggests that a direct interaction via the FERM domain of kindlerin is likely. We were unable to confirm that the FERM domain was responsible for this interaction because of the insolubility of C-terminal kindlerin fragments (data not shown) and the low expression of N-terminal kindlerin fragments (data not shown).

Reduction of kindlerin by siRNA resulted in delayed cell spreading. Adhesion was not affected by kindlerin knock-down when tested 30 min after replating on fibronectin or laminin (data not shown). Therefore, it is unlikely that kindlerin is required for integrin-ligand interaction. The biochemical interaction between kindlerin and the cytoplasmic domains of β integrins may contribute to efficient linkage of the extracellular matrix to the actin cytoskeleton via integrin adhesion receptors. Moreover, the fact that kindlerin expression does not lead to integrin activation suggests that the impact of kindlerin on cell spreading occurs after integrin-ligand binding. Whether kindlerin is affecting the formation of the actin cytoskeleton to enable cell spreading or the assembly of the extracellular matrix to build focal adhesion attachment sites remains to be elucidated.

The kindlerin gene was recognized by linkage analysis as being mutated in a rare skin disease called Kindler syndrome. This disease is characterized by acral blistering, photosensitivity, and diffuse poikiloderma with cutaneous atrophy (1, 3) and shares some similarities in its clinical presentation with two subtypes of junctional epidermolysis bullosa that are caused by mutations in α_6 or β_4 integrin genes (18, 19, 52). Similar skin blistering phenotypes have been described in mice with disrupted α_3 (53) (a major integrin partner for β_1 integrin in the basolateral membrane of keratinocytes), α_6 (54), and β_4 (55) integrin genes as well as in mice genetically modified to specifically knock-out β_1 integrin expression in skin (56, 57). Skin lesions of patients affected with Kindler syndrome have normal desmosomes, hemidesmosomes, and anchoring filaments, and the major defect lies in the organization of the basement membrane that shows extensive reduplication and disruption of the lamina densa (58, 59). Interestingly, microscopic examination of skin from the α_3 integrin null mice (60) and the conditional β_1 integrin null mice (56, 57) also revealed a disorganized basement membrane. The disruption of the integrity of the basement membrane caused by genetic defects in α_3 and β_1 integrin and kindlerin implicates these proteins in basement membrane assembly and maintenance and suggests that they are likely components of the same signaling pathway. TGF-β not only enhances kindlerin expression as shown in this report but also increases the abundance of integrins (61, 62) and extracellular matrix constituents such as fibronectin, collagen, and laminin (63–66). Therefore, it is reasonable to postulate that organization of the newly synthesized extracellular matrix components by integrin and kindlerin complexes may be an important step in TGF-β-stimulated cell motility. All four of the mutations identified in Kindler syndrome create truncated proteins that have lost the F3 subdomain of the FERM domain, and three of the four mutations generate products lacking both FERM domains and the PH domain. This finding suggests that the F3 subdomain in kindlerin is necessary for stabilization of the basement membrane through formation of integrin complexes.

Kindlerin has also been implicated in human cancer as it was found to be significantly overexpressed in 60% of lung and 70% of colon carcinomas tested (2). Despite the similar domain topology shared with Mig-2 and URP2, only kindlerin gene expression was found to be up-regulated (2). Interestingly, many colon cancers have increased levels of TGF-β expression (67), which suggests that kindlerin is a TGF-β-inducible protein *in vivo* and evokes the possibility that kindlerin is involved in tumor pathophysiology.

Acknowledgments—We thank Diana Lim for the expert graphics and Vera Tai for technical support.

REFERENCES

1. Jobard, F., Bouadjar, B., Caux, F., Hadj-Rabia, S., Has, C., Matsuda, F., Weissenbach, J., Lathrop. M., Prud'homme, J. F., and Fischer, J. (2003) *Hum. Mol. Genet.* **12,** 925–935
2. Weinstein, E. J., Bourner, M., Head, R., Zakeri, H., Bauer, C., and Mazzarella, R. (2003) *Biochim. Biophys. Acta* **1637,** 207–216
3. Siegel, D. H., Ashton, G. H., Penagos, H. G., Lee, J. V., Feiler, H. S., Wilhelmsen, K. C., South, A. P., Smith, F. J., Prescott, A. R., Wessagowit, V., Oyama. N., Akiyama. M., Al Aboud, D., Al Aboud, K., Al Githami, A., Al Hawsawi, K., Al Ismaily. A., Al-Suwaid, R., Atherton, D. J., Caputo, R., Fine, J. D., Frieden, I. J., Fuchs, E., Haber, R. M., Harada, T., Kitajima, Y., Mallory, S. B., Ogawa, H., Sahin, S., Shimizu, H., Suga, Y., Tadini, G., Tsuchiya, K., Wiebe, C. B., Wojnarowska, F., Zaghloul, A. B., Hamada, T., Mallipeddi, R., Eady, R. A., McLean, W. H., McGrath, J. A., and Epstein, E. H. (2003) *Am. J. Hum. Genet.* **73,** 174–187
4. Garcia-Alvarez, B., de Pereda, J. M., Calderwood, D. A., Ulmer, T. S., Critchley, D., Campbell, I. D., Ginsberg, M. H., and Liddington, R. C. (2003) *Mol. Cell* **11,** 49–58
5. Savagner, P. (2001) *BioEssays* **23,** 912–923
6. Thiery, J. P. (2002) *Nat. Rev. Cancer* **2,** 442–454
7. Akhurst, R. J., and Derynck, R. (2001) *Trends Cell Biol.* **11,** S44–S51
8. Derynck, R., Akhurst, R. J., and Balmain, A. (2001) *Nat. Genet.* **29,** 117–129
9. Oft, M., Heider, K. H., and Beug, H. (1998) *Curr. Biol.* **8,** 1243–1252
10. McEarchern, J. A., Kobie, J. J., Mack, V., Wu, R. S., Meade-Tollin, L., Arteaga, C. L., Dumont, N., Besselsen, D., Seftor, E., Hendrix, M. J., Katsanis, E., and Akporiaye, E. T. (2001) *Int. J. Cancer* **91,** 76–82
11. Janda, E., Lehmann, K., Killisch, I., Jechlinger, M., Herzig, M., Downward. J., Beug, H., and Grunert, S. (2002) *J. Cell Biol.* **156,** 299–314
12. Boland, S., Boisvieux-Ulrich, E., Houcine, O., Baeza-Squiban, A., Pouchelet, M., Schoevaert, D., and Marano, F. (1996) *J. Cell Sci.* **109,** 2207–2219
13. Bakin, A. V., Tomlinson, A. K., Bhowmick, N. A., Moses, H. L., and Arteaga, C. L. (2000) *J. Biol. Chem.* **275,** 36803–36810
14. Ellenrieder, V., Hendler, S. F., Boeck, W., Seufferlein, T., Menke, A., Ruhland, C., Adler, G., and Gress, T. M. (2001) *Cancer Res.* **61,** 4222–4228
15. Bhowmick, N. A., Ghiassi, M., Bakin, A., Aakre, M., Lundquist, C. A., Engel, M. E., Arteaga, C. L., and Moses, H. L. (2001) *Mol. Biol. Cell* **12,** 27–36
16. Kindler, T. (1954) *Br. J. Dermatol.* **66,** 104–111
17. Forman, A. B., Prendiville, J. S., Esterly, N. B., Hebert, A. A., Duvic, M., Horiguchi, Y., and Fine, J. D. (1989) *Pediatr. Dermatol.* **6,** 91–101
18. Vidal, F., Aberdam, D., Miquel, C., Christiano, A. M., Pulkkinen, L., Uitto, J., Ortonne, J. P., and Meneguzzi, G. (1995) *Nat. Genet.* **10,** 229–234
19. Pulkkinen, L., Kimonis, V. E., Xu, Y., Spanou, E. N., McLean, W. H., and Uitto, J. (1997) *Hum. Mol. Genet.* **6,** 669–674
20. Rogalski, T. M., Muilen, G. P., Gilbert, M. M., Williams, B. D., and Moerman, D. G. (2000) *J. Cell Biol.* **150,** 253–264
21. Karpf, A. R., Peterson, P. W., Rawlins, J. T., Dalley, B. K., Yang, Q., Albertsen, H., and Jones, D. A. (1999) *Proc. Natl. Acad. Sci. U. S. A.* **96,** 14007–14012
22. Miller, G. S., and Fuchs, R. (1997) *Comput. Appl. Biosci.* **13,** 81–87
23. Beckerle, M. C. (1986) *J. Cell Biol.* **103,** 1679–1687
24. Guex, N., and Peitsch, M. C. (1997) *Electrophoresis* **18,** 2714–2723
25. Peitsch, M. C. (1996) *Biochem. Soc. Trans.* **24,** 274–279
26. Peitsch, M. C. (1995) *Bio/Technology* **13,** 658–660
27. Vriend, G. (1990) *J. Mol. Graphics* **8,** 52- 56
28. Hooft. R. W., Vriend, G., Sander, C., and Abola, E. E. (1996) *Nature* **381,** 272
29. Calderwood, D. A., Zent, R., Grant, R., Rees, D. J., Hynes, R. O., and Ginsberg, M. H. (1999) *J. Biol. Chem.* **274,** 28071–28074
30. Massague, J. (1998) *Annu. Rev. Biochem.* **67,** 753–791
31. Christian, J. L., and Nakayama, T. (1999) *BioEssays* **21,** 382–390
32. Verrecchia, F., and Mauviel, A. (2002) *J. Investig. Dermatol.* **118,** 211–215
33. Derynck, R., and Zhang, Y. E. (2003) *Nature* **425,** 577–584
34. Gerwin, B. I., Keski-Oja, J., Seddon, M., Leclmer. J. F., and Harris, C. C.

(1990) *Am. J. Physiol.* **259,** L262–L269
35. Stampfer, M. R., Yaswen, P., Alhadeff, M., and Hosoda, J. (1993) *J. Cell. Physiol.* **155,** 210–221
36. Akimov, S. S., and Belkin, A. M. (2001) *J. Cell Sci.* **114,** 2989–3000
37. Claisse, D., Martiny, I., Chaqour, B., Wegrowski, Y., Petitfrere, E., Schneider, C., Haye, B., and Bellon, G. (1999) *J. Cell Sci.* **112,** 1405–1416
38. Burridge, K., and Chrzanowska-Wodnicka, M. (1996) *Annu. Rev. Cell Dev. Biol.* **12,** 463–518
39. Kramer, R. H., McDonald, K. A., and Vu, M. P. (1989) *J. Biol. Chem.* **264,** 15642–15649
40. Rahilly, M. A., Salter, D. M., and Fleming, S. (1991) *J. Pathol.* **165,** 163–171
41. Gates, R. E., Hanks, S. K., and King, L. E., Jr. (1993) *Biochem. J.* **289,** 221–226
42. Horiba, K., and Fukuda, Y. (1994) *Virchows Arch.* **425,** 425–434
43. Levy, L., Broad, S., Diekmann, D., Evans, R. D., and Watt, F. M. (2000) *Mol. Biol. Cell* **11,** 453–466
44. Bretscher, A., Edwards, K., and Fehon, R. G. (2002) *Nat. Rev. Mol. Cell. Biol.* **3,** 586–599
45. Pearson, M. A., Reczek, D., Bretscher, A., and Karplus, P. A. (2000) *Cell* **101,** 259–270
46. Calderwood, D. A., Yan, B., de Pereda, J. M., Alvarez, B. G., Fujioka, Y., Liddington, R. C., and Ginsberg, M. H. (2002) *J. Biol. Chem.* **277,** 21749–21758
47. Ulmer, T. S., Calderwood, D. A., Ginsberg, M. H., and Campbell, I. D. (2003) *Biochemistry* **42,** 8307–8312
48. Tadokoro, S., Shattil, S. J., Eto, K., Tai, V., Liddington, R. C., de Pereda, J. M., Ginsberg, M. H., and Calderwood, D. A. (2003) *Science* **302,** 103–106
49. Girault, J. A., Labesse, G., Mornon, J. P., and Callebaut, I. (1999) *Trends Biochem. Sci.* **24,** 54–57
50. Zavadil, J., Bitzer, M., Liang, D., Yang, Y. C., Massimi, A., Kneitz, S., Piek, E., and Bottinger, E. P. (2001) *Proc. Natl. Acad. Sci. U. S. A.* **98,** 6686–6691
51. Tu, Y., Wu, S., Shi, X., Chen, K., and Wu, C. (2003) *Cell* **113,** 37–47
52. Niessen, C. M., van der Raaij-Helmer, M. H., Hulsman, E. H., van der Neut, R., Jonkman, M. F., and Sonnenberg, A. (1996) *J. Cell Sci.* **109,** 1695–1706
53. Kreidberg, J. A. (2000) *Curr. Opin. Cell Biol.* **12,** 548–553
54. Georges-Labouesse, E., Messaddeq, N., Yehia, G., Cadalbert, L., Dierich, A., and Le Meur, M. (1996) *Nat. Genet.* **13,** 370–373
55. van der Neut, R., Krimpenfort, P., Calafat, J., Niessen, C. M., and Sonnenberg, A. (1996) *Nat. Genet.* **13,** 366–369
56. Brakebusch, C., Grose, R., Quondamatteo, F., Ramirez, A., Jorcano, J. L., Pirro, A., Svensson, M., Herken, R., Sasaki, T., Timpl, R., Werner, S., and Fassler, R. (2000) *EMBO J.* **19,** 3990–4003
57. Raghavan, S., Bauer, C., Mundschau, G., Li, Q., and Fuchs, E. (2000) *J. Cell Biol.* **150,** 1149–1160
58. Haber, R. M., and Hanna, W. M. (1996) *Arch. Dermatol.* **132,** 1487–1490
59. Shimizu, H., Sato, M., Ban, M., Kitajima, Y., Ishizaki, S., Harada, T., Bruckner-Tuderman, L., Fine, J. D., Burgeson, R., Kon, A., McGrath, J. A., Christiano, A. M., Uitto, J., and Nishikawa, T. (1997) *Arch. Dermatol.* **133,** 1111–1117
60. DiPersio, C. M., Hodivala-Dilke, K. M., Jaenisch, R., Kreidberg, J. A., and Hynes, R. O. (1997) *J. Cell Biol.* **137,** 729–742
61. Ignotz, R. A., and Massague, J. (1987) *Cell* **51,** 189–197
62. Koivisto, L., Larjava, K., Hakkinen, L., Uitto, V. J., Heino, J., and Larjava, H. (1999) *Cell Adhes. Commun.* **7,** 245–257
63. Garbi, C., Colletta, G., Cirafici, A. M., Marchisio, P. C., and Nitsch, L. (1990) *Eur. J. Cell Biol.* **53,** 281–289
64. Furuyama, A., Iwata, M., Hayashi, T., and Mochitate, K. (1999) *Eur. J. Cell Biol.* **78,** 867–875
65. Nguyen, N. M., Bai, Y., Mochitate, K., and Senior, R. M. (2002) *Am. J. Physiol.* **282,** L1004–L1011
66. Yi, J. Y., Hur, K. C., Lee, E., Jin, Y. J., Arteaga, C. L., and Son, Y. S. (2002) *Eur. J. Cell Biol.* **81,** 457–468
67. Bellone, G., Carbone, A., Tibaudi, D., Mauri, F., Ferrero, I., Smirne, C., Suman, F., Rivetti, C., Migliaretti, G., Camandona, M., Palestro, G., Emanuelli, G., and Rodeck, U. (2001) *Eur. J. Cancer* **37,** 224–233